Watershed Ecology and the Environment 4 (2022) 73–85

Contents lists available at ScienceDirect

Watershed Ecology and the Environment

journal homepage: www.keaipublishing.com/en/journals/watershed-ecology-

Assessment of water, soil contamination and land cover changes in Sims and Vince Bayou urban watersheds of Houston, Texas

Felica R. Davis [a], Maruthi Sridhar Balaji Bhaskar [b,*]

[a] Department of Environmental and Interdisciplinary Sciences, Texas Southern University, Houston, TX, USA
[b] Department of Earth and Environment, Florida International University, Miami, FL, USA

A R T I C L E I N F O

Article history:
Received 15 June 2022
Revised 22 August 2022
Accepted 23 August 2022
Available online 28 August 2022

Keywords:
Heavy metals
Land cover change
Nutrient
Pollution
Spatial distribution
Socio-economic characteristics

A B S T R A C T

Intense urbanization and increased industrialization in urban and suburban watersheds result in the decrease of vegetation and increase in impermeable surfaces contributing to the decline of soil and water quality. The goal of this study is to investigate the impact of urbanization and industrialization on urban watersheds. The specific objectives are to, 1) determine nutrient and heavy metal concentrations in soil and water samples along Sims Bayou (SB) and Vince Bayou (VB), 2) analyze land cover changes over the last 3 decades in each watershed and 3) evaluate socio-economic characteristics and human health risks within these watersheds. Triplicate soil and water samples were collected from downstream, midstream, and upstream locations during the fall and spring seasons along both bayous. The samples were analyzed to determine elemental concentrations using inductive coupled plasma mass spectrometer (ICP-MS) and total carbon and nitrogen (TCN) analyzer. Landsat 5 TM and Landsat 8 OLI/TIRS images were used to derive thematic land cover maps using ERDAS Imagine v16.5 software. The elemental concentrations were interpolated to spatial maps for distribution analysis using ESRI ArcGIS-10.8 software. The chemical analysis of water samples collected from SB and VB revealed that the N, P, Cu, Ni, Pb, and Zn concentrations were found at elevated levels that can pose threat for aquatic organisms. Among soil samples, the concentrations of Cr, Cu, Ni, Pb and Zn exceeded the levels of soil background concentrations of Texas. Land cover change patterns were similar for both watersheds with high vegetative surfaces decreasing and low vegetative surfaces increasing significantly over the past three decades. Both watersheds experienced an increase in total population with SB watershed increasing 27.9% and VB watershed increasing 9.1% from 1990 to 2020. Health risk assessments revealed risks for Cd, Cr, and Ni in soil via ingestion for children under age 6 in both bayous. This research is critical in improving our understanding on the impact of natural and human activities on Houston watersheds.

1. Introduction

Heavy metals and metalloids are naturally occurring elements having a high atomic weight and a density greater than 5.0 g cm^{-3} (Tchounwou et al., 2012). The various anthropogenic sources of heavy metals as well as their toxic, persistent and bio accumulative nature raises concern over the potential effects on human health and the environment. Factors influencing toxicity are dependent on the dose, route of exposure, chemical species, and the age, gender, genetics, and nutritional status of exposed individuals (Ali et al., 2019). Because of their high degree of toxicity, Pb, Cd, Hg, Cr and As are listed as priority pollutants by the Environmental Protection Agency (EPA) (Wuana and Okieimen, 2011). Heavy metals can enter water bodies by industrial and consumer waste, or through leaching of metals from soil and releasing them into streams, lakes, rivers, and groundwater. To a lesser extent, they enter our bodies via food, drinking water and air (Tchounwou et al., 2012). Heavy metal sources include mining and petrochemical industries, industrial production, untreated sewage sludge and varied other sources such as metal piping, traffic, and combustion by-products from coal-burning power stations (Dibofori-Orji et al., 2019). It is, therefore, important to assess and monitor the concentrations of potentially toxic heavy metals in various environmental media. This study provides an analysis of the occurrence of heavy metals in soil and water measured over two different time periods across different watersheds in Southeastern Texas.

* Corresponding author at: Department of Earth and Environment, Florida International University, Miami, FL 33199, USA.

E-mail address: mbalajib@fiu.edu (M.S.B. Bhaskar).

https://doi.org/10.1016/j.wsee.2022.08.002
2589-4714/

Water is designated as the "life-blood of the biosphere" because its properties contribute to the suitability of Earth as an environment for life (Ali et al., 2019). Heavy metals are one of the most hazardous pollutants in water and have been found in various water bodies such as lakes (Zeng and Wu, 2013), rivers and reservoirs (Xia et al., 2018) resulting in deterioration of water quality. They can be observed in the dissolved phase (Shotyk et al., 2017), suspended particle phase (Rügner et al., 2019), and sedimentary phases (Li et al., 2019a, Li et al., 2019b) in water systems. The dissolved phase heavy metals are generally more toxic than the other two phases (Shotyk et al., 2017).

Soil is the most critical interface in an ecosystem as it can be a source of pollution to surface water, ground water, sediment and living organisms (Xu et al., 2013). Major sources of soil heavy metal pollution include industrial and municipal effluent, fertilizers, and pesticides. Heavy metal sources have different characteristics and patterns of contaminations depending on the land use patterns (Gaw et al., 2006). Soil type as well as its physical and chemical parameters can also affect levels of elemental concentrations significantly. Comprehensive understanding of factors that affect heavy metal residues in soils will help in understanding the fate of metals in soils and in the examination of possible methods of remediation of contaminated soils. The Texas Commission on Environmental Quality (TCEQ) has developed water quality criteria in the Texas Surface Water Quality Standards (TSWQS) for metals (TCEQ, 2021). The TSWQS establish explicit goals for the quality of streams, rivers, lakes, and bayous throughout the state. Standards are developed to maintain the quality of surface waters in Texas so that it supports public health, recreation and protects aquatic life, consistent with the sustainable economic development of the state.

Land cover is the surface components of land on earth such as vegetation, water, soil, living organisms, and other structural features created by human activities (Gao and O'Neill, 2020). Land cover change (LCC) is one of the most observable, rapid, irreversible, and impactful changes occurring in urban and suburban watersheds. Urbanization, deforestation, mining, extensive agricultural practices, and economic growth are the main influences on land cover conversions (Popov et al., 2021). The need has arisen to manage the urban environment sustainably because of rapid population growth and the increased ability to access and utilize natural resources (Gao and O'Neill, 2020). The rates and trends of LCC are factors affecting discharge and water quality in watersheds. These changes can affect stream flow, surface runoff, infiltration rate, ground water recharge and water quality (Popov et al., 2021).

Surface runoff is a major source of water pollution especially during severe storm events. Water runs along land surfaces picking up litter, chemicals, fertilizers, and other toxic substances that can harm an entire ecosystem. There are several factors contributing to the amount of runoff in an area including rainfall amount, vegetation, soil type, shape and size of catchment, and land use (USGS, 2019). The decrease in vegetative surfaces results in high surface runoff and low water retention in watersheds (Sulamo et al., 2021). Vegetative surfaces can slow down the flow of runoff and allow more time for infiltration into the soil. Therefore, studying the impacts of land cover change is crucial to solving a variety of problems, including the design of hydraulic structures, urban and highway drainage, flood-control planning, source pollution, and the evaluation of other environmental impacts (Sulamo et al., 2021). Significant increase in urban impervious surfaces along with reduction of vegetative surfaces was seen in Brays, Buffalo, and Greens Bayou watersheds of Houston (Bukunmi-Omidiran and Sridhar, 2021; Sridhar et al., 2020).

The goal of this research is to comprehensively assess land cover changes and development density in correlation with nutrient and metal pollution in surface soils and water of Sims and Vince Bayou watersheds. The specific objectives are to, 1) determine nutrient and heavy metal concentrations in soil and water samples along Sims Bayou (SB) and Vince Bayou (VB), 2) analyze land cover changes over the last 3 decades in each watershed and 3) evaluate socio-economic characteristics and human health risks within these watersheds.

2. Materials and methods

2.1. Description of study areas

This study was conducted in the humid subtropical climate region of Greater Houston located in Southeast Texas. Two urban watersheds, Sims Bayou Watershed (SBW) and Vince Bayou Watershed (VBW), were assessed to determine the level of heavy metal contamination, amount of land cover change, socio-economic dynamics, and human health risk from heavy metal exposure. The SBW and VBW (Fig. 1) are highly developed urban watersheds located in the southern region of Harris County (HCFCD, 2021). The SBW covers approximately 243 square kilometers and has two major streams (Sims and Berry Bayous). This watershed has a long history of flooding where structural flooding has damaged many homes along Sims Bayou and its tributaries during numerous storm events (HCFCD, 2020a). The VBW covers about 41.4 square kilometers and includes two main streams, Vince Bayou, and Little Vince Bayou. The existing floodplains of this watershed has produced out-of-bank flooding conditions under many severe storm events (HCFCD, 2020b).

The typical flora of the SBW and VBW include several mature stands of coastal floodplain hardwood forests, along with woody shrubs and smaller trees serving as understory. The tree canopy provides shelter for various wading birds and raptors while the thickets and tall grasses, provide habitat for songbirds, migrating warblers and sparrows (HCFCD, 2020a; 2020b). The weedy habitat provides cover for caterpillars and adult butterflies.

2.2. Data collection and analysis

Soil and water samples were collected in fall of 2020 and spring of 2021from three separate locations along Sims and Vince Bayous. Samples were identified by an abbreviated bayou name followed by its distance (in kilometers) from mouth of the bayou. The downstream, midstream, and upstream locations for Sims Bayou (SB) and Vince Bayou (VB) were labeled as SB2.2, SB16.9, SB36.1 and VB0.9, VB5.1, VB6.4, respectively. Soil and water samples were collected in triplicate from each sample locations and the geographic coordinates were recorded using a portable GPS device. Sample preparation and analysis followed methods 3051A and 3015A (EPA, 2020). Results obtained from the water and soil sample analysis were compared with Ecological Screening Benchmarks (TCEQ, 2021) and Nutrient Criteria of Rivers & Streams (EPA, 2021b) to identify chemicals of concern.

Land cover change analysis provides valuable information for studying topographic changes for rapidly growing metropolitan areas. Landsat satellite imageries were selected for the periods of 1984, 1994, 2004, 2014 and 2020 for the land cover change analysis. The details of the downloaded satellite imagery are given in Table 1. Images for the study areas were orthorectified to a Universal Transverse Mercator projection using datum WGS (World Geodetic System) 84 zone 15 N using ERDAS Imagine v16.5 software prior to classification.

The Normalized Difference Vegetation Index (NDVI) is essential in identifying the vegetation cover in remotely sensed data obtained from space borne sensors (USGS, 2021). This index is

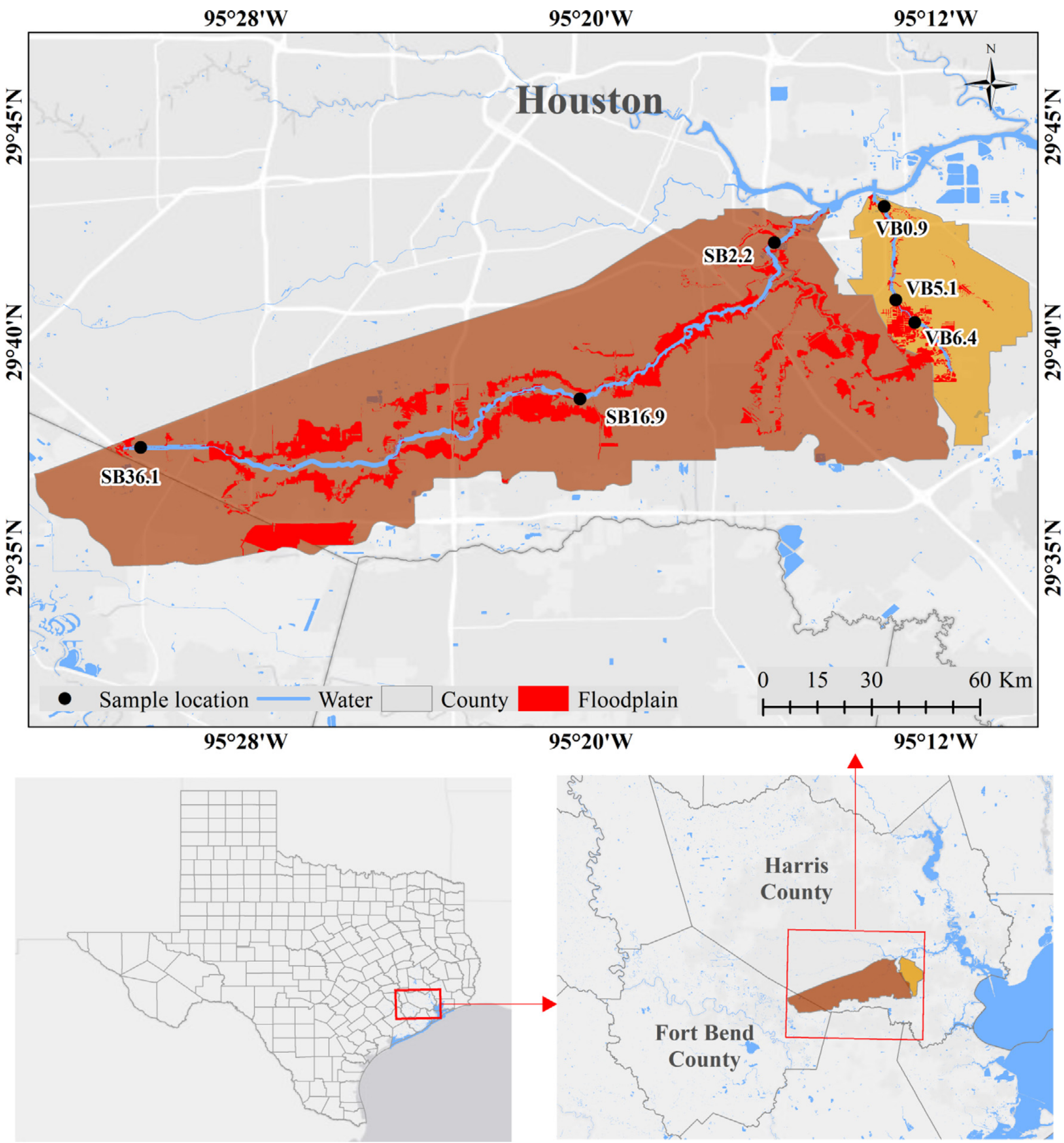

Fig. 1. The Sims and Vince Bayou watersheds along with sample locations and 500-year floodplain.

Table 1
Landsat images used in this study.

Sensor	File name	Acquisition date	Cloud Cover	Path/Row
TM	LT50250391984342XXX02	12/7/1984	0%	25/39
TM	LT50250391994353XXX02	12/19/1994	0%	25/39
TM	LT50250392004349EDC00	12/14/2004	0%	25/39
OLI	LC80250392014328LGN01	11/24/2014	0%	25/39
OLI	LC80250392020361LGN00	12/26/2020	0%	25/39

helpful in the analysis of spatial and temporal changes in vegetation coverage. NDVI is expressed as: NDVI = (Band 4 – Band 3) / (Band 4 + Band 3) for Landsat TM images and NDVI = (Band 5 – Band 4) / (Band 5 + Band 4) for Landsat OLI images. The NDVI values ranging from −1 to 1 was used to reclassify the imagery and divide into water, no vegetation, low vegetation, and high vegetation classes as shown in Table 2. Maximum likelihood and supervised classification algorithm based on the NDVI threshold method was used to generate land cover thematic maps. The classification results were evaluated using accuracy assessment. Reference data including Google earth images, true and false color combination images and base knowledge of the study areas were

Table 2
Land cover classes along with the NDVI values used for classification of Landsat TM and OLS imagery.

Class name	NDVI value	Description
Water	−1 to −0.1	Water body
No vegetation	−0.1 to 0.099	Built-up area
Low vegetation	0.1 to 0.199	Sparse vegetation
High vegetation	0.2 to >1	Dense vegetation

used for verification purposes and to generate a classification error matrix. The land cover maps were evaluated for overall accuracy, kappa coefficient, producer, and user's accuracies.

Social, demographic, and economic dynamics plays a vital role in spatial and temporal land use and land cover conversions. Land use and land cover conversions are necessary and important for continued economic development and social progress. Therefore, population data was collected for census years 1990 and 2020 to assess the socio-environmental interactions related to urbanization. Various health problems in urban areas arise from environmental conditions, so it is crucial to monitor environmental hazards and human health outcomes. Health risks of heavy metals in soil from SBW and VBW via ingestion, inhalation, and dermal contact were evaluated based on the United States Environmental Protection Agency (USEPA) risk assessment method. Children are more susceptible to the effects of heavy metals than adults. Health risks for children via ingestion, inhalation, and dermal contact is calculated using the equations below:

$$ADD_{ingest} = \frac{CxIgRxEFxEDxCF}{BWxAT}$$

$$ADD_{dermal} = \frac{CxSAxAFxABSxEFxEDxCF}{BWxAT}$$

$$ADD_{inhale} = \frac{CxIhRxEFxED}{PEFxBWxAT}$$

where *C* is the concentration of the HM of interest in soil (mg/kg); *IgR* is the ingestion rate of soil (mg/day); *EF* is the exposure frequency (350 days); *ED* is the exposure duration (6 years); *CF* is the conversion factor (1×10^{-6} kg/mg); *BW* is body weight (15 kg); and *AT* is the average lifetime (*ED* × 365 days and 70 × 365 days for non-carcinogenic and carcinogenic, respectively). For dermal exposure risk, *SA* is the exposed skin area (2,800 cm^2); *AF* is the skin adherence factor for soil (0.2 for child $mg/cm^2/day$), and *ABS* is the dermal absorption factor from the soil (chemical-specific). For inhalation, *IhR* is the inhalation rate (7.6 m^3/day); and *PEF* is particulate emission factor (1.36×10^9 m^3/kg).

Carcinogenic risks are estimated to determine the probability of developing cancer over a lifetime of exposure (Yadav, et al., 2019). CR values $<1 \times 10^{-4}$ indicate low risk, values between 1×10^{-4} and 1×10^{-3} are tolerable risks while values exceeding $1x10^{-3}$ are considered unacceptable risk (Ge et al., 2013). CR risk is calculated using the equation, Cancer risk (CR) = ADD × CSF.

3. Results

Nutrient and metal elemental concentrations detected in water and soil samples for SB and VB are shown in Table 3. For water samples, the concentrations of Cu, Zn, P, and TDN were at levels that can affect aquatic life. The mean Cu concentrations of water at SB (0.57–3.30 μg L^{-1}) and VB (2.67–3.13 μg L^{-1}) were above chronic aquatic life protection levels (0.96 μg L^{-1}). Zn concentrations in water for both SB (2.93–24.4 μg L^{-1}) and VB (0.00–12.9 μg L^{-1}) exceeded chronic aquatic life protection levels of 0.99 μg L^{-1}. All water samples revealed high concentrations for P at both SB (56.3–862 μg L^{-1}) and VB (146–1829 μg L^{-1}) that exceeded the nutrient criteria level set at 36.56 μg L^{-1}. The mean TDN concentrations for water samples at SB (697–3313 μg L^{-1}) and VB (815–4229 μg L^{-1}) were above the nutrient criteria level of 690 μg L^{-1}. Correlations among elemental concentrations in water samples are given in Table 4. Pearson correlation coefficients for SB water samples revealed very strong (r = 0.90–1.0) and highly significant ($p < 0.01$) positive correlations between P and TDN concentrations. For VB, correlations among elemental concentrations of water samples revealed very strong (r = 0.90–1.0) and highly significant ($p < 0.01$) positive correlations between P with Zn and TDN (Table 4). Strong (r = 0.70–0.89) and highly significant ($p < 0.01$) positive correlations were revealed between Ni with Zn, P and TDN as well as between Zn and TDN (Table 4) concentrations of water samples. Moderate (r = 0.40–0.69) and significant ($p < 0.05$) positive correlation was found between Cd and Ni (Table 4) concentrations in VB water samples.

The mean metal concentrations in soil samples, background concentrations and ecological benchmarks associated with ecological risk assessments for soils is shown in Table 3. The mean concentrations of Cr, Cu, Ni, Pb, and Zn were above background levels in most soil samples (Table 3). The Cr concentration at the downstream (SB2.2) location for SB (31.5 mg kg^{-1}) and the midstream (VB5.1) location for VB (24.6–35.8 mg kg^{-1}) exceeded background and terrestrial plants protection levels. The Cu concentrations at the midstream (SB16.9) location for SB (27.08 mg kg^{-1}) and the downstream (VB0.9) and upstream (VB6.4) locations for VB (29.0 and 25.3 mg kg^{-1}, respectively) exceeded soil background levels of 15 mg kg^{-1}. Ni concentrations at the downstream (SB2.2) and midstream (SB16.9) locations for SB (13.3 and 12.5 mg kg^{-1}, respectively) and at the midstream (VB5.1) and upstream (VB6.4) locations for VB (15.0 and 17.3 mg kg^{-1}, respectively) exceeded soil background levels of 10 mg kg^{-1}. The Pb concentrations at the midstream (SB16.9) location for SB (18.0 mg kg^{-1}) and at all sample locations for VB (19.5–31.7 mg kg^{-1}) exceeded background levels of 15 mg kg^{-1}. Zn concentrations at all sample locations for SB (34.4–120 mg kg^{-1}) and VB (90.1–111 mg kg^{-1}) exceeded its corresponding background level (30 mg kg^{-1}). However, Pb and Zn concentrations were not at levels that can affect terrestrial plants. Correlations among metals in soil samples are presented in Table 5. For SB, Pearson correlation coefficients revealed very strong (r = 0.90–1.0) and highly significant ($p < 0.01$) positive correlations between Cr and Ni, between Cu with P and TDN, and between Pb and Zn (Table 5). There were also strong (r = 0.70–0.89) and highly significant ($p < 0.01$) positive correlations between Cd with Cr and Ni, between Cu with Pb and Zn, and between Zn and TDN (Table 5). Moderate (r = 0.40–0.69) and significant ($p < 0.01$) positive correlation was found between Pb with Cd, P and TDN and between Zn and P (Table 5). Finally, there was moderate (r = 0.40–0.69) and significant ($p < 0.05$) positive correlation between Cd and Zn and between Ni with Cu and Pb (Table 5). Pearson correlation coefficients for VB revealed strong (r = 0.70–0.89) and highly significant ($p < 0.01$) positive correlations between Cr and Cd. Moderate (r = 0.40–0.69) and significant ($p < 0.01$) positive correlation was found between Cd and Ni and between TDN with Cd and Ni. However, there was moderate (r = 0.40–0.69) and highly significant ($p < 0.05$) negative correlation between Cu with Cd and TDN (Table 5).

3.1. Soil enrichment and spatial distribution patterns of nutrients and heavy metals

3.1.1. Sims Bayou

Enrichment of metals in soil samples collected from Sims Bayou was estimated as shown in Fig. 2. Based on the enrichment factor (EF) calculations, overall enrichment values decreased as follows:

Table 3
Metal concentrations in water (μg L^{-1}) and soil (mg kg^{-1}) samples (n = 18) for Sims and Vince Bayou.

Metal	Media	SB2.2	SB16.9	SB36.1	VB0.9	VB5.1	VB6.4	ALP	HHP	EPA	Plant	BG
Cd	**Water**	0.03	BDL	0.08	0.08	0.12	BDL	**1.10**	**5**	–	–	–
	Soil	1.02	0.91	0.52	0.61	1.01	0.73	–	–	–	**32**	**1**
Cr	**Water**	0.15	0.20	0.63	BDL	0.57	0.33	**10.6**	**62**	–	–	–
	Soil	31.5	29.2	19.4	26.2	35.8	24.6	–	–	–	**1**	**30**
Cu	**Water**	0.57	2.40	3.30	2.67	2.77	3.13	**0.96**	–	–	–	–
	Soil	12.4	27.1	9.64	29.0	13.6	25.3	–	–	–	**70**	**15**
Ni	**Water**	BDL	0.62	BDL	1.43	BDL	BDL	**1.00**	**332**	–	–	–
	Soil	13.3	12.5	7.64	7.33	15.0	17.3	–	–	–	**38**	**10**
Pb	**Water**	0.90	BDL	BDL	0.97	BDL	1.28	**1.46**	**1.15**	–	–	–
	Soil	14.9	18.0	7.48	31.7	22.7	19.5	–	–	–	**120**	**15**
Zn	**Water**	2.93	24.4	14.9	12.9	BDL	BDL	**0.99**	–	–	–	–
	Soil	84.0	120	34.4	90.1	97.5	111	–	–	–	**160**	**30**
P	**Water**	108	862	56.30	1829	146	150	–	–	**36.6**	–	–
	Soil	198	883	135	437	305	285	–	–	–	–	–
TDN	**Water**	1289	3313	697	4229	815	952	–	–	**690**	–	–
	Soil	1017	3152	913	982	2713	1845	–	–	–	–	–

Note: Below Detectable Level (BDL); Chronic = Chronic levels for Aquatic Life Protection (ALP); Human Health Protection (HHP); EPA criteria for aggregate nutrients (EPA). Toxicological benchmarks for screening contaminants of potential concern for effects on terrestrial plants (Plant); Texas-Specific Soil Background Concentrations (BG).

Table 4
Correlation among variables in water samples (n = 18) for Sims and Vince Bayou.

Sims Bayou							
	Cd	Cr	Cu	Ni	Pb	Zn	P
Cr	0.33						
Cu	−0.05	−0.07					
Ni	−0.11	−0.17	0.26				
Pb	−0.11	0.30	−0.21	−0.06			
Zn	0.14	−0.12	0.27	0.08	−0.20		
P	−0.29	0.02	−0.02	0.01	−0.04	−0.05	
TDN	−0.35	−0.02	−0.05	0.04	0.02	−0.20	0.98**
Vince Bayou							
	Cd	**Cr**	**Cu**	**Ni**	**Pb**	**Zn**	**P**
Cr	0.25						
Cu	0.22	0.12					
Ni	0.58*	−0.21	0.32				
Pb	0.20	0.23	0.33	0.34			
Zn	0.35	−0.35	0.14	0.74**	0.26		
P	0.34	−0.33	0.21	0.76**	0.22	0.92**	
TDN	0.39	−0.32	0.29	0.87**	0.18	0.85**	0.94**

Notes: Levels of significance: * $p < 0.05$; ** $p < 0.01$; TDN = Total Dissolved Nitrogen.

Table 5
Correlation among variables in soil samples (n = 18) for Sims and Vince Bayou.

Sims Bayou							
	Cd	Cr	Cu	Ni	Pb	Zn	P
Cr	0.87**						
Cu	0.45	0.34					
Ni	0.89**	0.92**	0.47*				
Pb	0.69**	0.35	0.74**	0.49*			
Zn	0.56*	0.21	0.78**	0.33	0.95**		
P	0.33	0.21	0.93**	0.34	0.66**	0.69**	
TDN	0.37	0.28	0.92**	0.38	0.65**	0.70**	0.98**
Vince Bayou							
	Cd	**Cr**	**Cu**	**Ni**	**Pb**	**Zn**	**P**
Cr	0.75**						
Cu	−0.52*	−0.16					
Ni	0.61**	0.21	−0.35				
Pb	−0.18	0.06	0.06	−0.39			
Zn	−0.11	−0.19	0.31	0.13	0.13		
P	−0.10	−0.28	0.04	−0.25	0.14	−0.05	
TDN	0.62**	0.32	−0.54*	0.61**	−0.06	0.05	0.15

Notes: Levels of significance: * $p < 0.05$; ** $p < 0.01$; TDN = Total Dissolved Nitrogen.

Zn > Ni > Cu > Cr > Pb > Cd. Results showed that Zn was significantly (5 ≤ EF < 20) enriched while Cd, Cr, Cu, Ni, and Pb showed moderate enrichment (2 ≤ EF < 5) in soil samples. The distribution of heavy metals in water and soil samples exhibited varied spatial patterns as shown in Fig. 3. The soil concentrations of Pb, P and N remained higher in the midstream (SB16.9) location compared to the other locations along the bayou (Fig. 3). The P and N concentration in the water samples of SB were higher in the midstream (SB16.9) location compared to the other locations along the bayou, while the Pb concentrations in the water showed no trend. The Pb concentrations in soil samples were correlated with the moderate (2 ≤ EF < 5) enrichment at the midstream (SB16.9) location of SB (Fig. 2).

3.1.2. Vince Bayou

The degree of enrichment of metals in soil samples is shown in Fig. 4. Based on the enrichment factor (EF) calculations, overall enrichment values decreased as follows: Zn > Cu > Pb > Ni > Cr > Cd. Results showed that Cu, Pb and Zn showed significant enrichment (5 ≤ EF < 20) in soil samples while Cd, Cr, and Ni showed moderate enrichment (2 ≤ EF < 5). Spatial distribution of heavy metals in water and soil samples for VB are shown in Fig. 5. Lead concentrations did not show significant variation in water samples but spatial patterns in soil samples indicated higher concentrations at the downstream (VB0.9) location (Fig. 5) compared to other locations. The water and soil concentrations of P and N showed higher concentrations in the downstream (VB0.9) location (Fig. 5) compared to others. In soil, Cu, Pb, and Zn concentrations were correlated with the very high (20 ≤ EF < 40) enrichment levels at the downstream location (VB0.9) of VB.

3.1.3. Land cover change analysis

The land cover maps for the watersheds were generated for years 1984, 1994, 2004, 2014, and 2020 using the Normalized Difference Vegetation Index (NDVI) threshold approach. NDVI values were divided into four main classes including Water, No vegetation, Low vegetation, and High vegetation. Accuracy assessment for both Sims Bayou and Vince Bayou watersheds was greater than 90% while Kappa coefficient greater than 0.70 indicating substantial accuracy (Table 6).

Land cover changes in SBW and VBW for years 1984 and 2020 are shown in Fig. 6. Image classification results showed that the total land area of SBW was approximately 248 sq. km. High vegetative surfaces decreased by 71.7% over the past 3 decades losing an estimated 135.06 sq. km. while low vegetative surfaces increased by 360.9% from 32.06 sq. km. in 1984 to 147.78 sq. km. in 2020. The change in Water class was also very significant as it increased in total area from 1.00 sq. km. in 1984 to 3.07 sq. km. in 2020. Non-vegetative surfaces increased by 60.3% from 27.51 sq. km. in 1984 to 44.10 sq. km. in 2020.

Image classification results showed that the total land area of VBW was approximately 40.0 sq. km. High vegetative surfaces decreased by 73.2% while low vegetative surfaces increased by 233.2%. The change in Water class was also very significant as it increased in total area from 0.09 sq. km. in 1984 to 0.43 sq. km. in 2020. Non-vegetative surfaces increased by 35.7% from 6.89 sq. km. in 1984 to 23.04 sq. km. in 2020.

3.1.4. Socio-economic dynamics

The total population in the SBW increased by 27.9% from 334,279 residents in 1990 to 427,599 residents in 2020 (Fig. 7). Densely populated areas are mostly found in the eastern region of the watershed with a few in the western region as shown in Fig. 7. There are significantly smaller populated areas in the Central region of the watershed. For census year 1990, the racial composition in the SBW shows that 42.6% of residents were identified as Black, 29.0% Hispanic residents, 25.6% White residents, 2.5% Asian residents and 0.3% all other races (Fig. 7). However, according to the 2020 census SBW experienced a significant shift in racial diversity. By census year 2020 Hispanic residents accounted for 56.5% of the total population while Asian and all other race residents slightly increased to 2.6% and 1.7%, respectively (Fig. 7). However, there was a decrease in both Black (33.6%) and White (5.5%) residents in the watershed. The median household income for the watershed increased from $24,531 in 1990 to $47,188 in 2020 as shown in Fig. 7 but stayed below the Texas median income for both years.

The total population of the VBW increased by 9.1% from 110,640 residents to 120,729 residents in 2020. Small densely populated areas are found in the northern and southern regions of the watershed as shown in Fig. 8. There is a significantly smaller populated area in the Northern region of the watershed closer to the Houston Ship Channel. For census year 1990, the racial composition in the watershed shows that 63.9% of residents were identified

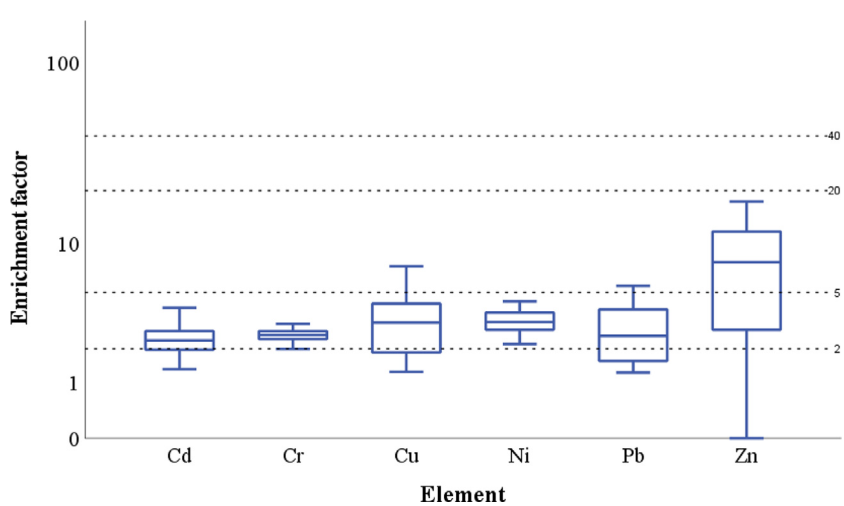

Fig. 2. Soil enrichment of heavy metals at Sims Bayou. * The top and bottom of each box represent 75th and 25th percentiles respectively, line across inside of each box represents median, and asterisk beyond whiskers are outliers.

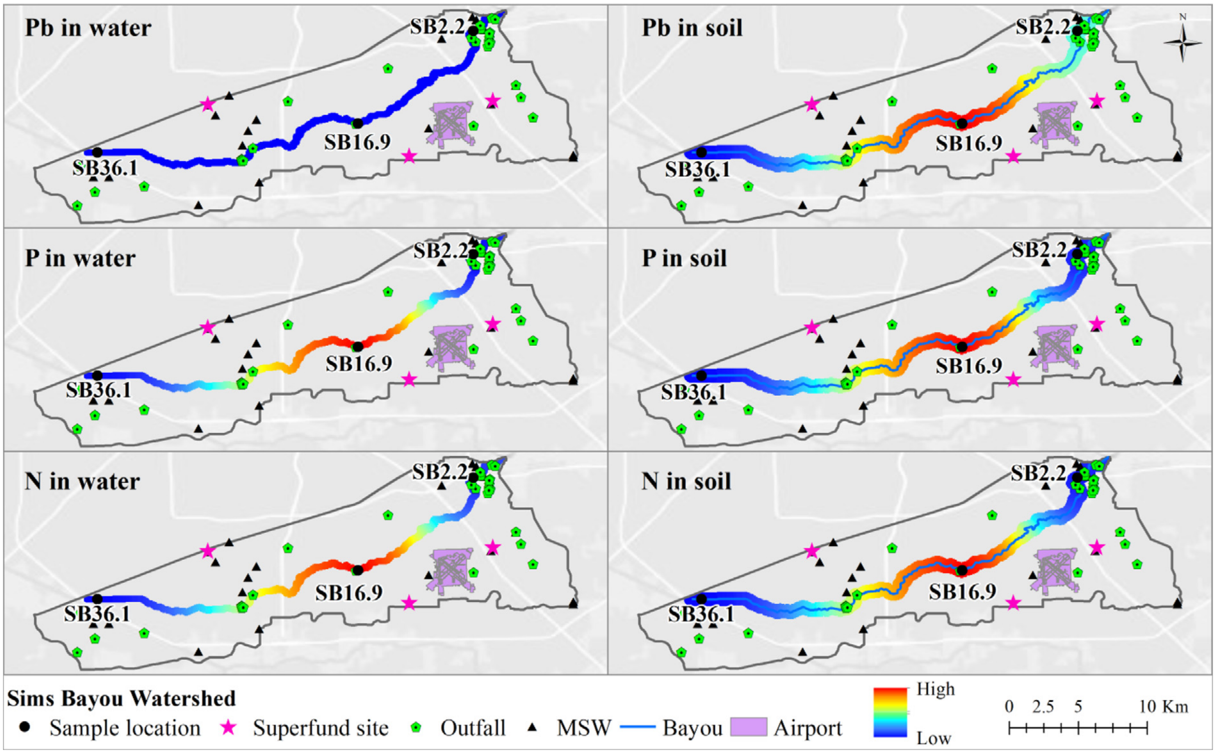

Fig. 3. Spatial distribution of Pb, P and N and in water (μg L^{-1}) and soil (mg kg^{-1}) samples of Sims Bayou Watershed (SBW). Outfalls = Wastewater Outfalls, MSW = Municipal Solid Waste Facilities.

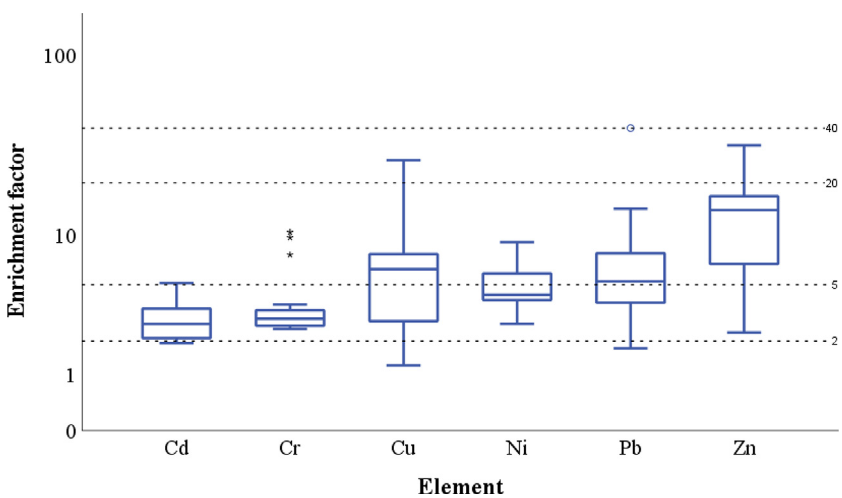

Fig. 4. Soil enrichment of heavy metals at Vince Bayou. * The top and bottom of each box represent 75th and 25th percentiles respectively, line across inside of each box represents median, and asterisk beyond whiskers are outliers.

as White, 32.4% Hispanic residents, 2.0% Asian residents, 1.1% Black residents and 0.5% all other races. On the other hand, the 2020 census shows the highest percentage for Hispanic residents (78.9%), 15.0% White residents, 3.5% Black residents, 1.1% Asian residents and 1.6% all other residents. The demographic percentage by race is shown in Fig. 8. The median household income for the watershed increased from $25,095 in 1990 to $47,798 in 2020 as shown in Fig. 8, which remains below the Texas median income for both years.

3.1.5. Health risk assessment of heavy metals in surface soils

Three major exposure pathways are considered for the human health risk assessment including ingestion, dermal absorption, and inhalation. Results of the non-carcinogenic and carcinogenic health risks posed by six priority heavy metals (Cd, Cr, Cu, Ni, Pb, and Zn) are shown in Table 7. Hazard index (HI) values were<1 for both Sims and Vince Bayou soils indicating no significant risk of non-carcinogenic effects. However, the LCR and TLCR values for Cd, Cr and Ni were greater than $1x10^{-4}$ indicating risks for carcinogenic effects via ingestion. Carcinogenic health risks were found for SB and VB. In soils collected from SBW, health risks values for Cd, Cr, and Ni at the downstream (SB2.2) location were 1.61 to 2.15 times greater than acceptable levels (Table 7) while values at the upstream (SB36.1) location displayed the lowest risks with levels 1.04 to 1.32 times greater than acceptable cancer risk level (Table 7). Therefore, the cancer risks values and site location levels

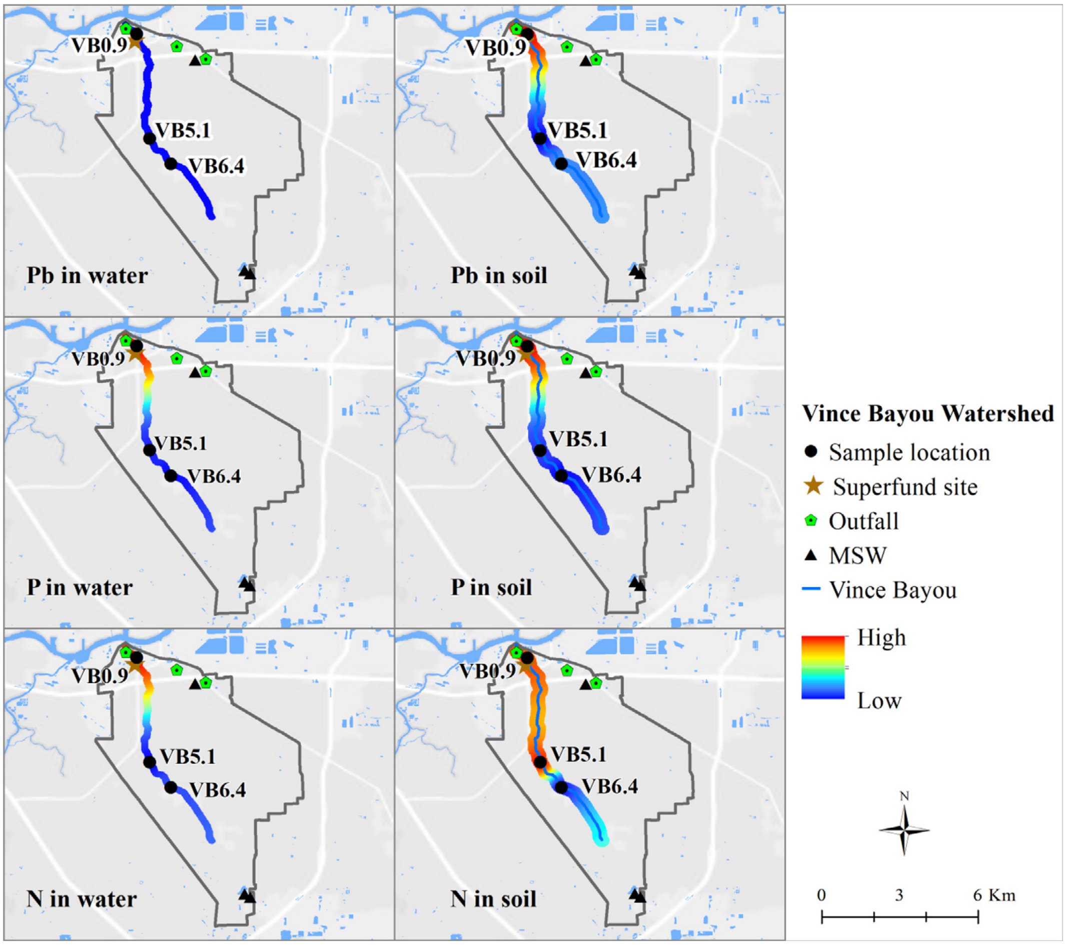

Fig. 5. Spatial distribution of Pb, P and N in water (μg L^{-1}) and soil (mg kg^{-1}) samples from Vince Bayou Watershed (VBW). Outfalls = Wastewater Outfalls, MSW = Municipal Solid Waste Facilities.

Table 6
Accuracy Assessment of vegetation maps in 1984 and 2020 for Sims and Vince Bayou.

Sims Bayou	**Land Cover Map 1984**		**Land Cover Map 2020**	
Land Cover Classes	PA%	UA%	PA%	UA%
Water	100%	75%	100%	97%
No vegetation	87%	87%	96%	92%
Low vegetation	75%	93%	91%	94%
High vegetation	99%	95%	90%	90%
Overall Accuracy	**92%**		**93%**	
Kappa Coefficient	**0.74**		**0.89**	
Vince Bayou	**Land Cover Map 1984**		**Land Cover Map 2020**	
Land Cover Classes	PA%	UA%	PA%	UA%
Water	100%	75%	100%	85%
No vegetation	82%	86%	93%	93%
Low vegetation	72%	73%	95%	93%
High vegetation	96%	98%	85%	96%
Overall Accuracy	**89%**		**93%**	
Kappa Coefficient	**0.82**		**0.89**	

Note: Producer Accuracy (PA) and User's Accuracy (UA).

in decreasing order are Cr > Cd > Ni and SB2.2 > SB16.9 > SB36.1, respectively for SBW. Soil samples collected from VBW showed health risk values greater than $1x10^{-4}$ for Cd and Cr for the mid-stream (VB5.1) location at 2.03 to 2.44 times greater than acceptable levels (Table 7) while values for Ni at the upstream (VB6.4) location displayed the highest risk with levels 2.10 to 2.15 times greater than acceptable cancer risk level (Table 7). The cancer risk values and site location levels in decreasing order for VBW are Cr > Cd > Ni and VB5.1 > VB6.4 > VB0.9, respectively.

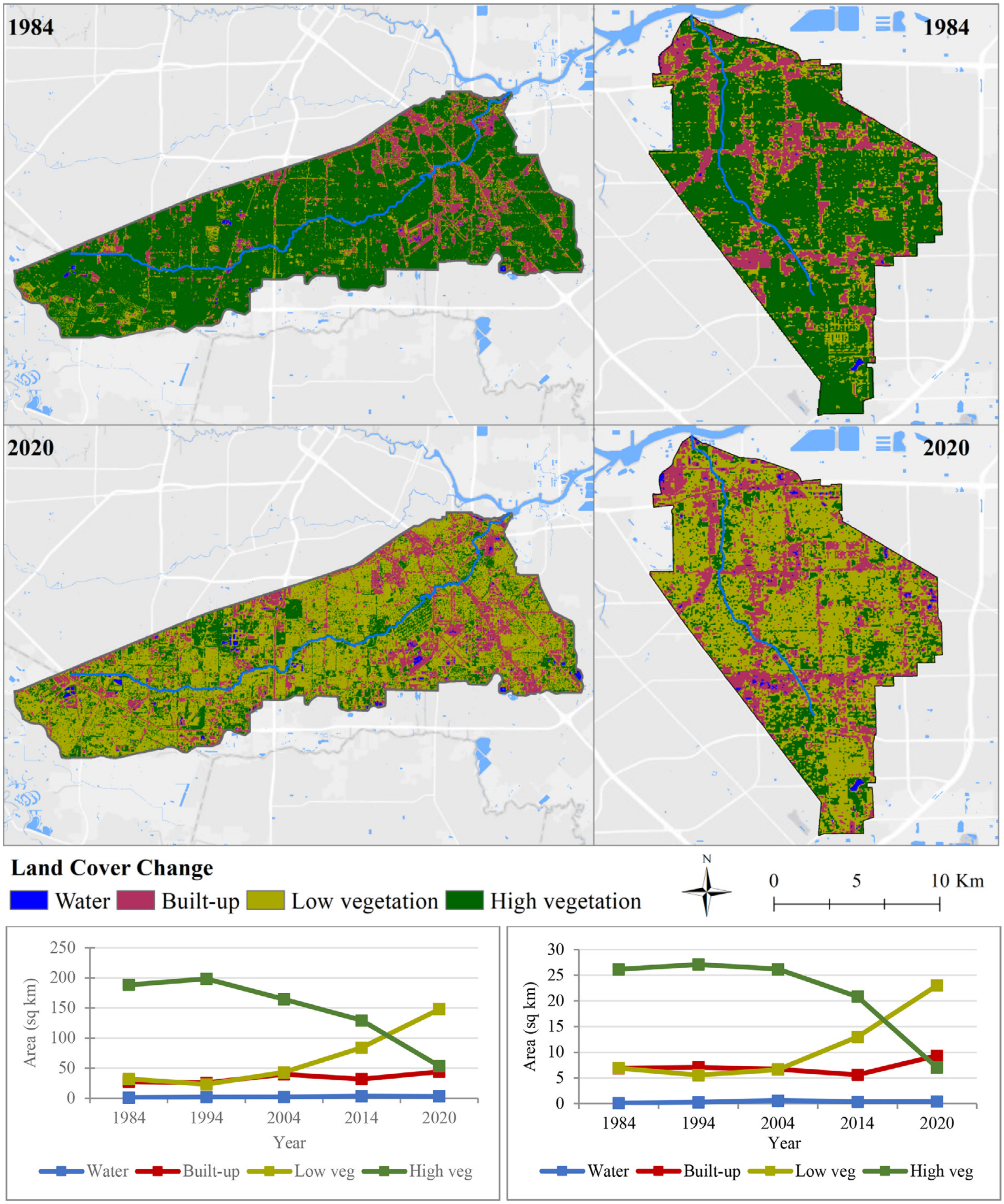

Fig. 6. Land cover map of Sims Bayou and Vince Bayou watersheds for (a) 1984, (b) 2020, and (c) land cover change from 1984 to 2020.

4. Discussion

4.1. Heavy metal pollution of water and soil

The chemical analysis of water samples showed that the elements of concern affecting aquatic organisms were Cu, Zn, P, and TDN in Sims Bayou and Cu, Ni, Pb, Zn, P, and TDN in Vince Bayou. In aquatic organism, very low concentrations of heavy metals can induce oxidative stress (Singh and Kalamdhad, 2011). The concentrations of Cu, Ni, Pb, Zn, P and TDN in water samples were higher than the levels for aquatic life and human health protection. Copper is ubiquitous in the environment and found in rocks, soil, water, and air. At trace amounts Cu is essential for specific protein enzyme functions. Increased industrial and agricultural activities have amplified Cu concentrations that enter aquatic systems (NCBI, 2022). Copper concentrations in Sims Bayou (0.57–3.30 μg L^{-1}) and Vince Bayou (2.67–3.13 μg L^{-1}) exceeded acute (lethal) and chronic (sublethal) levels set for the protection of aquatic life (0.96 μg L^{-1}) in over 72% of the water samples collected. Chronic effects of Cu include reduced growth, immune response, reproduc-

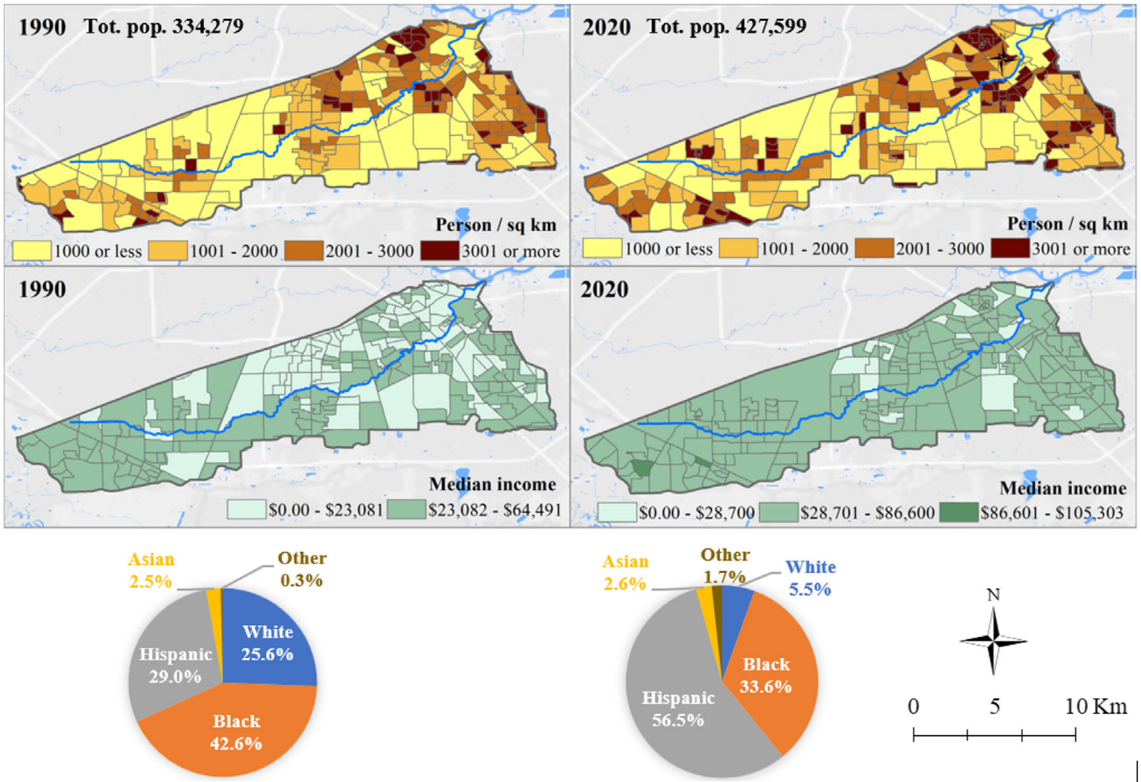

Fig. 7. Population density, ethnicity composition and population race distribution in Sims Bayou watershed (SBW) for census years of 1990 and 2020.

tion and/or survival in aquatic organisms (The Nature Conservancy, 2011). Nickel concentrations (0–1.43 μg L^{-1}) in water samples at VB downstream (VB0.9) location slightly exceeded acute and chronic (1.0 μg L^{-1}) levels set for aquatic life protection (EPA, 2021b). Lethal and sublethal effects include survival outcomes, reduced growth and impaired reproduction and metabolism (Patuxent Wildlife Research Center, 1998). The Pb concentrations (0.00–1.28 μg L^{-1}) in water samples exceeded human health protection level (1.15 μg L^{-1}) in samples collected at the upstream (VB6.4) location (EPA, 2021b). Human exposure to Pb can result in toxicity effects including kidney and reproduction dysfunction, inhibition of the synthesis of hemoglobin and teratogenic effects (Singh and Kalamdhad, 2011). The concentrations of Zn (0–24.4 μg L^{-1}) in water samples exceeded acute (0.98 μg L^{-1}) and chronic (0.99 μg L^{-1}) levels set for the protection of aquatic life at all sample locations for Sims Bayou but only at the downstream (VB0.9) locations for Vince Bayou. Acute effects of Zn can cause fish kills by destroying gill tissues and chronic toxic effects can induce stress resulting in death (Li, et al., 2019). Mean P (56.3–1,829 μg L^{-1}) and TDN (697–4,229 μg L^{-1}) concentrations in all the water samples collected were above the nutrient criteria level of 690 μg L^{-1} and 36.56 μg L^{-1}. Excess phosphorus and nitrogen in the water can impair water quality, food resources, and decrease dissolved oxygen needed for aquatic life survival (EPA, 2021a). Some algal blooms can produce elevated toxins and bacterial growth that are harmful to humans encounter the polluted water, consume tainted fish, shellfish, or drink contaminated water (EPA, 2021a).

In soil samples, Cr, Cu, Ni, Pb and Zn exceeded their corresponding background values found in Texas-specific soil (TCEQ, 1999) for most of the samples collected. The concentrations for Cr were also at levels that can affect soil invertebrates and/or terrestrial plants. The Cr concentrations (19.4–35.8 mg kg^{-1}) in soil samples collected from the downstream (SB2.2) location for SB and the midstream (VB5.1) location for VB were significantly higher. Soil Cr concentrations above 1 mg kg^{-1} for plants can cause harmful effects (TCEQ, 2021). In plants, Cr can induce oxidative stress and lipid peroxidation thereby causing severe damage to cell membranes (Asati, 2016). The spatial distribution of heavy metals in water and soil sample collected from SB were highest at the midstream (SB16.9) location which closely correlated with the numerous upstream municipal solid waste sites and wastewater outfalls. Higher heavy metal and nutrient concentrations in soil samples collected from VB was at the midstream (VB5.1) location, compared to other locations.

4.2. Land cover change analysis and Socio-economic dynamics

Over the last four decades, the most significant changes occurred within the regions classified as high and low vegetative surfaces. In the landcover class of high vegetative surface, the area decreased by 71.7% in SBW while VBW experienced a 73.2% decrease. Non-vegetative surfaces increased in both SBW and VBW by 60.3% and 35.7%, respectively. The increase in the impervious surfaces are a result of intensive residential development and the extension of road networks within these watersheds. The U.S. Census data (Manson et al., 2021) revealed a boom in population for each watershed from 1990 to 2020. The largest population increase occurred in the SBW with 27.9% while VBW increased by 9.1%. Both watersheds have shown a gradual large-scale emigration of White residents leading to racial or ethnic shifts. For example, white residents in the VBW decreased from 63.9% in census year 1990 to 15.0% by 2020 and SBW decreased from 25.6% to 5.5%. These watersheds have a majority minority population as of census year 2020. In urban areas, problems such as overcrowding, ethnocultural diversity and physical deterioration of areas with large dense populations are thought to contribute to the emigration of white residents (i.e., white flight or exodus) (Kye, 2018).

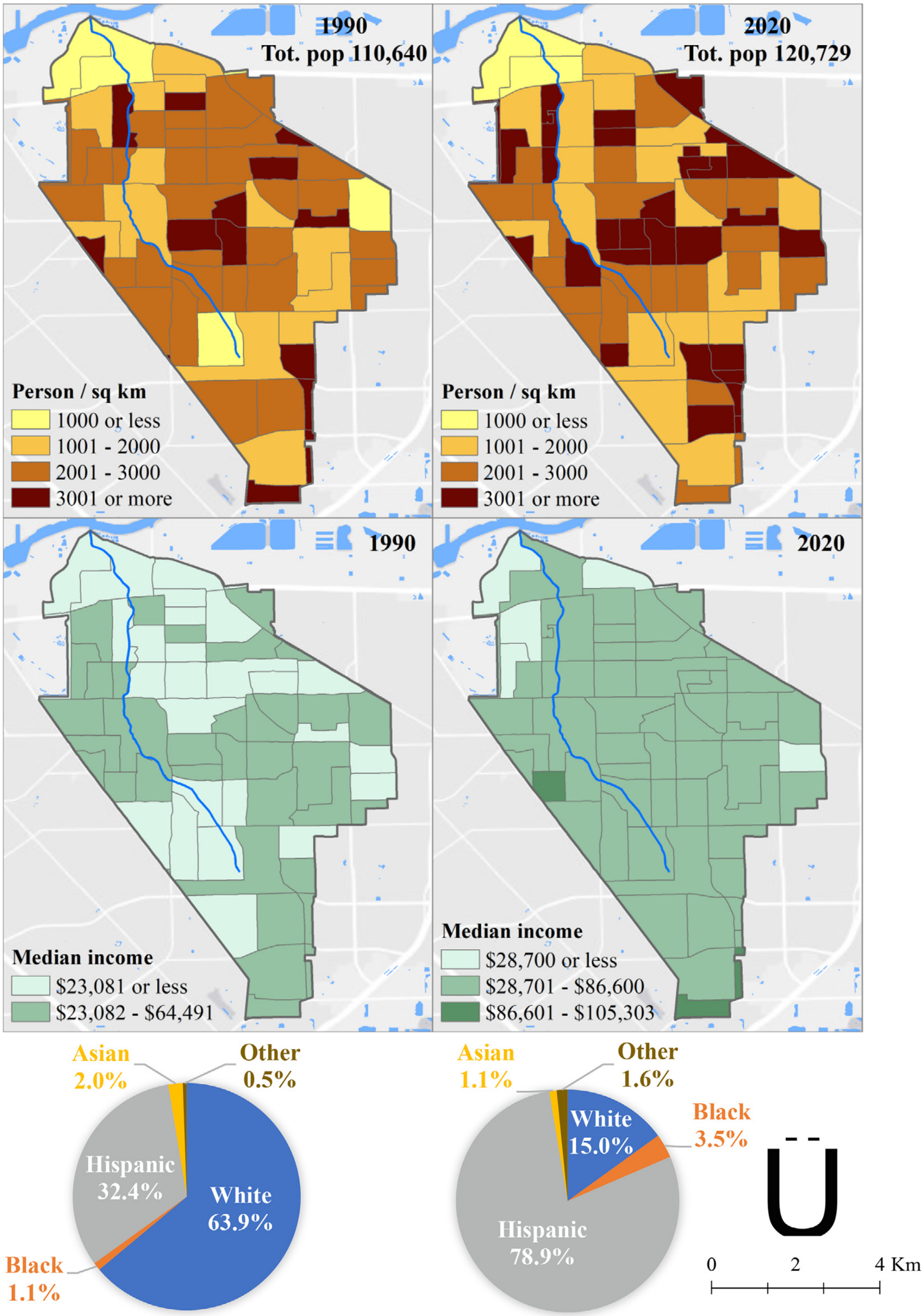

Fig. 8. Population density, ethnicity composition and income distribution in Vince Bayou watershed (VBW) for census year 1990 and 2020.

Income levels for residents in these urban watersheds were at or below the median income reported for Texas residents as of census year 2020.

4.3. Risk assessment analysis

Children under the age of 6 years are most susceptible to long-term cancer risks from heavy metal exposure (Cui et al., 2018). Other harmful effects include mental retardation, neurocognitive disorders, behavioral disorders, respiratory problems, and cardiovascular diseases (Osman et al., 2019). The health risk assessment revealed that cancer risks at SBW and VBW exceeded the acceptable level ($1x10^{-4}$) for children from ingestion of soil contaminated with Cd, Cr, and Ni. Risk levels for soil samples collected at VBW range from $1.21x10^{-4}$ to $2.44x10^{-4}$ and at SBW risk range from $1.04x10^{-4}$ to $2.15x10^{-4}$. Health risks from exposure to Cd include

Table 7
Carcinogenic risk of priority heavy metals in soil from Sims and Vince Bayou Watersheds (SBW, VBW) for children under 6 years of age.

Element	Risk	SB2.2	SB16.9	SB36.1	VB0.9	VB5.1	VB6.4
Cd	**Hazard index (HI)**	1.40E−01	1.24E−01	7.08E−02	8.29E−02	1.38E−01	9.99E−02
	LCR dermal	4.78E−06	4.26E−06	2.42E−06	2.84E−06	4.74E−06	3.42E−06
	LCR ingestion	2.05E−04	1.82E−04	1.04E−04	1.21E−04	2.03E−04	1.46E−04
	LCR inhalation	1.29E−09	1.15E−09	6.54E−10	7.65E−10	1.28E−09	9.22E−10
	TLCR	2.09E−04	1.86E−04	1.06E−04	1.24E−04	2.08E−04	1.50E−04
Cr	**Hazard index (HI)**	1.43E−01	1.33E−01	8.83E−02	1.19E−01	1.63E−01	1.12E−01
	LCR dermal	4.90E−06	4.55E−06	3.02E−06	4.08E−06	5.58E−06	3.83E−06
	LCR ingestion	2.10E−04	1.95E−04	1.29E−04	1.75E−04	2.39E−04	1.64E−04
	LCR inhalation	1.32E−09	1.23E−09	8.14E−10	1.10E−09	1.50E−09	1.03E−09
	TLCR	2.15E−04	1.99E−04	1.32E−04	1.79E−04	2.44E−04	1.68E−04
Ni	**Hazard index (HI)**	9.20E−03	8.69E−03	5.30E−03	5.08E−03	1.04E−02	1.20E−02
	LCR dermal	3.76E−06	3.55E−06	2.17E−06	2.08E−06	4.25E−06	4.91E−06
	LCR ingestion	1.61E−04	1.52E−04	9.27E−05	8.89E−05	1.82E−04	2.10E−04
	LCR inhalation	1.02E−09	9.58E−10	5.84E−10	5.60E−10	1.15E−09	1.33E−09
	TLCR	1.65E−04	1.56E−04	9.49E−05	9.10E−05	1.86E−04	2.15E−04

Note: LCR, Lifetime cancer risk; TLCR, Total lifetime cancer risk. Underline: Values that exceeded the acceptable level, HI more than 1 and CRs greater than 1.00E−04.

renal damage, osteoporosis, pediatric cancer, cardiovascular diseases, and stunted growth (Osman, et al., 2019). Health effects from ingestion of Cr include cancer and adverse gastrointestinal, hematological, immune, kidney and liver effects (Osman et al., 2019). The most common effect from Ni exposure is allergic reactions. Individual that are highly sensitive to Ni may experience an allergic reaction after consuming food or water or breathe dust containing Ni (ATSDR, 2005).

5. Conclusion

Our chemical analysis revealed that the Cu, Ni, Pb, Zn, P and N in water samples collected from SB and VB were found to be at levels that can pose a threat for aquatic organisms. Higher metal concentrations in water samples were found in SB compared to concentrations found in VB. In soil samples, Cr, Cu, Ni, Pb and Zn were significantly enriched compared to the background levels occurring naturally in Texas soils, particularly in the SB. Intense urbanization and industrialization in both watersheds have contributed to the deterioration of soil and water quality. Overall land cover change patterns were similar for both watersheds with vegetative surfaces decreasing significantly while impervious surfaces increased over the past three decades. The increase in impervious surfaces correlated with rapid population growth indicating urban expansion throughout the region. Land cover changes was significant with SBW having the higher conversion of vegetative surfaces compared to VBW. Both watersheds experienced extensive population growth with SBW adding 3111 residents per year and VBW adding 336 residents per year over a 30-year period from 1990 to 2020. The watersheds were shown to have mostly minority residents who earn less than the median household income reported for the state of Texas. Human Health Risk Assessments were calculated to determine the individuals most at risk from exposure to heavy metal pollution. Results revealed that Cd, Cr, and Ni being the primary metals of concern for children under age 6 years. Health risks were found to be higher in VB compared to the risk revealed at SB This study helps in understanding how rapid urbanization and industrialization contribute to soil and water pollution in the Bayous of Houston metropolis and the long-term consequences on the environment.

Declaration of Competing Interest

The authors declare that they have no known competing financial interests or personal relationships that could have appeared to influence the work reported in this paper.

Acknowledgments

We acknowledge Djene Keita for the chemical analysis of soil and water samples and the SURE undergraduate student interns for helping in soil and water sampling. This research was primarily supported by the National Science Foundation (NSF) through the Texas Southern University (TSU) under the award numbers HRD-1829184 and BCS-1831205.

References

Ali, H., Khan, E., Ilahi, I., 2019. Environmental chemistry and ecotoxicology of hazardous heavy metals: environmental persistence, toxicity, and bioaccumulation. J Chem., 1–14.
ATSDR, 2005. Nickel. U.S. Department of Health and Human Services, Atlanta. https://www.atsdr.cdc.gov/toxfaqs/tfacts15.pdf.
Bukunmi-Omidiran, T., Maruthi Sridhar, B.B., 2021. Evaluation of spatial and temporal water and soil quality in the Buffalo and Brays Bayou watersheds of Houston, Texas. Remote Sens. Appl.: Soc. Environ. 21: 1-13. 100455. https://doi.org/10.1016/j.rsase.2020.100455.
The Nature Conservancy., 2011. Effects of Copper on Fish and Aquatic Resources. https://www.conservationgateway.org/ConservationByGeography/NorthAmerica/UnitedStates/alaska/sw/cpa/Documents/W2013ECopperF062012.pdf
Cui, Z., Wang, Y., Zhao, N., Yu, R., Xu, G., Yu, Y., 2018. Spatial distribution and risk assessment of heavy metals in paddy soils of yongshuyu irrigation area from Songhua River Basin, North- east China. Chin. Geogr. Sci. 25 (5), 797–809. https://doi.org/10.1007/s11769-018-0991-1.
Dibofori-Orji, A., Ihunwo, O., Udo, K., Shahabinia, A., Onyema, M., Mmom, P., 2019. Spatial and temporal distribution and contamination assessment of heavy metal in Woji Creek. Environ. Res. Commun. 1 (11), 1–10. https://doi.org/10.1088/2515-7620/ab4a8c.
EPA., 2021a. Nutrient Pollution. https://www.epa.gov/nutrientpollution/.
EPA., 2021b. Summary Table for the Ecoregional Nutrient Criteria Documents. .
EPA., 2020. The SW-846 Compendium. https://www.epa.gov/hw-sw846/sw-846-compendium.
Gao, J., O'Neill, B., 2020. Mapping global urban land for the 21st century with data-driven simulations and Shared Socioeconomic Pathways. Nat. Commun. 11 (2302), 1–12. https://doi.org/10.1038/s41467-020-15788-7.
Gaw, S., Wilkins, A., Kim, N., Palmer, G., Robinson, P., 2006. Trace element and Sigma DDT concentrations in horticultural soils from the Tasman, Waikato and Auckland regions of New Zealand. Sci. Total Environ. 355, 31–47. https://doi.org/10.1016/j.scitotenv.2005.02.020.
HCFCD., 2020a. Find Your Watershed. https://www.hcfcd.org/Find-Your-Watershed/Sims-Bayou.
HCFCD., 2020b. Find Your Watershed. https://www.hcfcd.org/Find-Your-Watershed/Vince-Bayou.
HCFCD., 2021. Don't know your watershed? https://www.hcfcd.org/.
Kye, S., 2018. The persistence of white flight in middle-class suburbia. Soc. Sci. Res. 72, 38–52.
Li, R., Tang, C., Li, X., Jiang, T., Shi, Y., Cao, Y., 2019a. Reconstructing the historical pollution levels and ecological risks over the past sixty years in sediments of the Beijing River, South China. Sci. Total Environ. 649, 448–460. https://doi.org/10.1016/j.scitotenv.2018.08.283.

Li, X., Wang, P., Feng, C., Liu, D., Chen, J., Wu, F., 2019b. Acute Toxicity and Hazardous Concentrations of Zinc to Native Freshwater Organisms Under Different pH Values in China. Bull. Environ. Contam. Toxicol. 103 (1), 120–126. https://doi.org/10.1007/s00128-018-2441-2.

Manson, S., Schroeder, J., Van Riper, D., Kugler, T., Ruggles, S., 2021. IPUMS National Historical Geographic Information System: Version 16.0. https://www.nhgis.org.

NCBI., 2022. https://pubchem.ncbi.nlm.nih.gov/compound/Copper.

Osman, M., Yang, F., Massey, I., 2019. Exposure routes and health effects of heavy metals on children. Biometals 32 (4), 563–573.

Patuxent Wildlife Research Center, 1998. Nickel Hazards To Fish, Wildlife, And Invertebrates: A Synoptic Review. U.S. Geological Survey, Laurel.

Popov, M., Michaelides, S., Stankevich, S., Kozlova, A., Piestova, I., Lubskiy, M., Titarenko, O., Svideniuk, M., Andreiev, A., Ivanov, S., 2021. Assessing long-term land cover changes in watershed by spatiotemporal fusion of classifications based on probability propagation: The case of Dniester river basin. Remote Sens. Appl.: Soc. Environ. 22, 1–13. https://doi.org/10.1016/j.rsase.2021.100477.

Rügner, H., Schwientek, M., Milačič, R., Zuliani, T., Vidmar, J., Paunović, M., Laschou, S., Kalogianni, E., Skoulikidis, N.T., Diamantini, E., Majone, B., Bellin, A., Chiogna, G., Martinez, E., Alda, M.L., Diaz-Cruz, M.S., Grwathwohl, P., 2019. Particle bound pollutants in rivers: Results from suspended sediment sampling in Globaqua River Basins. Sci. Total Environ. 647, 645–652. https://doi.org/10.1016/j.scitotenv.2018.08.027.

Shotyk, W., Bicalho, B., Cuss, C., Donner, M., Grant-Weaver, I., Haas-Neill, S., Javed, M.B., Krachler, M., Noernberg, T., Pelletier, R., Zaccone, C., 2017. Trace metals in the dissolved fraction (<0.45 µm) of the lower Athabasca River: Analytical challenges and environmental implications. Sci. Total Environ. 580, 660–669. https://doi.org/10.1016/j.scitotenv.2016.12.012.

Singh, J., Kalamdhad, A., 2011. Effects of heavy metals on soil, plants, human health and aquatic life. Int. J Res. Chem. Environ. 1 (2), 15–21.

Sridhar, B.B.M., Johnson, J., Mosuro, A., 2020. Impact of land cover changes on the soil and water quality of Greens Bayou watershed. Wat. Air and Soil Pollut. 231 (510). https://doi.org/10.1007/s11270-020-04890-7.

Sulamo, M., Kassab, A., Roba, N., 2021. Evaluation of the impacts of land use/cover changes on water balance of Bilate watershed, Rift valley basin. Ethiopia. Water Pract. Technol. 16 (4), 1108–1127. https://doi.org/10.2166/wpt.2021.063.

TCEQ., 1999. Subchapter C: Affected Property Assessment. https://www.tceq.texas.gov/assets/public/legal/rules/rules/pdflib/350c.pdf.

TCEQ., 2021. 2018 Texas Surface Water Quality Standards. https://www.tceq.texas.gov/assets/public/waterquality/standards/tswqs2018/2018swqs_allsections_nopreamble.pdf.

Tchounwou, P., Yedjou, C., Patlolla, A., Sutton, D., 2012. Heavy Metals Toxicity and the Environment. Exp. Suppl. 101, 133–164. https://doi.org/10.1007/978-3-7643-8340-4_6.

USGS., 2019. Surface Runoff and the Water Cycle. https://www.usgs.gov/special-topics/water-science-school/science/surface-runoff-and-water-cycle.

USGS., 2021. Landsat Normalized Difference Vegetation Index. https://www.usgs.gov/landsat-missions/landsat-normalized-difference-vegetation-index.

Wuana, R., Okieimen, F., 2011. Heavy metals in contaminated soils: a review of sources, chemistry, risks and best available strategies for remediation. ISRN Ecol.. https://doi.org/10.5402/2011/402647.

Xia, F., Qu, L., Wang, T., Luo, L., Chen, H., Dahlgren, R., Zhang, M., Mei, K., Huang, H., 2018. Distribution and source analysis of heavy metal pollutants in sediments of a rapid developing urban river system. Chemosphere 218–228. https://doi.org/10.1016/j.chemosphere.2018.05.090.

Xu, L., Wang, T., Luo, W., Ni, K., Liu, S., Wang, L., Li, Q., Lu, Y., 2013. Factors influencing the contents of metals and As in soils around the watershed of Guanting Reservoir, China. J. Environ. Sci. 561–568. https://doi.org/10.1016/s1001-0742(12)60095-3.

Zeng, H., Wu, J., 2013. Heavy metal pollution of lakes along the mid-lower reaches of the Yangtze River in China: Intensity, sources and spatial patterns. Int. J Environ. Res. Public Health. 10 (3), 793–807. https://doi.org/10.3390/ijerph10030793.